After recognizing the associative coefficient matrices, Danilevskii's method was used to evaluate each of these determinants. The results is

$$\frac{\partial|\lambda I-A|}{\lambda K}=(\lambda^4+6\lambda^3+11\lambda^2+6\lambda+2)-(\lambda^4+6\lambda^3+11\lambda^2+6\lambda) \tag{13}$$

or

$$\frac{\partial|\lambda I-A|}{\partial K}=2.0 \tag{14}$$

Thus,

$$\frac{\partial\lambda}{\partial K}=\frac{-2}{4\lambda^3+48\lambda^2+142\lambda+116} \tag{15}$$

Evaluating Eq. (15) at the roots of the characteristic equation, the sensitivity coefficients can be obtained.

Appendix

Danilevskii's method is a recursive technique for transforming any square matrix to the Forbenius form, i.e.,

$$P=\begin{bmatrix} 0 & 0 & \cdots & 0 & -d_0 \\ 1 & 0 & \cdots & 0 & -d_1 \\ 0 & 1 & \cdots & 0 & -d_2 \\ \vdots & \vdots & & & \\ 0 & 0 & & 1 & -d_{n-1} \end{bmatrix} \tag{A1}$$

Since the transformation is similar, the characteristic polynomials of Eq. (A1) and the original matrix are the same. It is easily verified that the characteristic polynomial of Eq. (A1) is

$$\Delta(\lambda)=|\lambda I-P|=\lambda^n+d_{n-1}\lambda^{n-1}+d_{n-2}\lambda^{n-2}+\ldots+d_0 \tag{A2}$$

The recurrence process is as follows:

$$A_{k+1}=S_k^{-1}A_kS_k \qquad k=1,2,\ldots,n-1 \tag{A3}$$

The matrix to be transformed to the Frobenius form is A; thus, $A_1=A$. The matrix S_k is formed from the identity matrix by replacing the $(k+1)$th column by the kth column of A_k. The matrix, S_k^{-1} is formed from the identity matrix by replacing the $(k+1)$th column by the negative of the kth column of A_k divided by the $(k+1)$th element except for the $(k+1)$th element, which is the positive reciprocal.

The recurrence process above suggests matrix operations. However, these operations are so simple that the kth step of the process can be described as follows:

$$b_{ij}=\begin{cases} a_{ij}/a_{ik} & \text{for } i=k+1 \\ a_{ij}-a_{ik}b_{k+1,j} & \text{for } i\neq k+1 \end{cases} \tag{A4}$$

and

$$a'_{ij}=\begin{cases} \sum_{\ell=1}^{n} b_{i\ell}a_{\ell k} & \text{for } j=k+1 \\ b_{ij} & \text{for } j\neq k+1 \end{cases} \tag{A5}$$

where $i=1,2,\ldots,n$, and $j=1,2,\ldots,n$; a_{ij} are the elements of the matrix A_k; a'_{ij} are the elements of the matrix A_{k+1}; b_{ij} are the elements of a "scratch-pad" matrix. The above are repeated $n-1$ times. For more details on implementing Danilevskii's method, see Refs. 6 and 7.

Acknowledgment

This work was partially supported by NASA, MSFC, Contract No. NAS8-31568.

References

[1] Van Ness, J. E., Boyle, J. M., and Imad, F. P., "Sensitivities of Large, Multi-Loop Control Systems," *IEEE Transactions on Automatic Control*, Vol. AC-10, July 1965, pp. 308-315.

[2] Morgan, B. S., Jr., "Sensitivity Analysis and Synthesis of Multivariable Systems," *IEEE Transactions on Automatic Control*, Vol. AC-11, July 1966, pp. 506-512.

[3] Reddy, D. C., "Evaluation of the Sensitivity Coefficient of an Eigenvalue," *IEEE Transactions on Automatic Control*, Vol. AC-12, Dec. 1967, p. 792.

[4] Rogers, L. C., "Derivatives of Eigenvalues and Eigenvectors," *AIAA Journal*, Vol. 8, May 1970, pp. 943-944.

[5] Rudisill, C. S. and Chu, Yee-Yeen, "Numerical Methods for Evaluating the Derivatives of Eigenvalues and Eigenvectors," *AIAA Journal*, Vol. 13, June 1975, pp. 834-837.

[6] Fadeev, D. K. and Fadeeva, V. N., *Computational Methods of Linear Algebra*, Freeman, San Francisco, Calif., 1963.

[7] Mitchell, Jerrel R., McDaniel, Willie L., and Nail, James B., "Control System Design by Pole Encouragement," Final Report, Contract No. NAS8-31568, NASA, MSFC, Sept. 3, 1976, pp. 68-76.

Contaminants in a Gasdynamic Mixing Laser

P. Hoffmann,* H. Hügel,† and W. Schall†
DFVLR, Institut für Technische Physik, Stuttgart, West Germany

Introduction

THE great potential of the gasdynamic mixing laser (GDML) as a high-energy system has been demonstrated by several groups, e.g., Refs. 1-4, to list but some of the more recent work. The basic idea that lies behind this conception is to produce separately thermally excited nitrogen and to inject cold carbon dioxide into a downstream region of lower temperature. By this means, advantage is taken of the facts that 1) the stagnation temperature can be raised to values far higher than the dissociation limit of CO_2, and 2) the freezing efficiency of a pure N_2-flow is extremely high. As a consequence, the available vibrational energy may be increased by approximately an order of magnitude as compared with typical values of premixed gasdynamic lasers (GDL).

In the work pertaining to the GDML, the nitrogen so far has been heated either in arc-heaters or in shock tubes. Both methods are useful and convenient in the course of basic investigations but may not be adequate in some applications. In those cases, a production of the hot N_2 by chemical means would be preferable. On the other hand, each combustion process yields products in addition to N_2, which might have adverse effects upon the molecular kinetics involved in the GDML.

The effect of some contaminating additives like O_2, NO, CO, SO_2, and H_2 on small signal gain and laser power of a small-scale GDML has been investigated experimentally and is reported in this Note.

Experiments and Discussions

The experimental apparatus used in this work is described in more detail in Ref. 4. Briefly, the N_2 is heated in a d.c. arc-

Received May 3, 1977; revision received June 16, 1977.
Index categories: Lasers; Thermochemistry and Chemical Kinetics.
*Research Scientist.
†Research Scientist, Member AIAA.

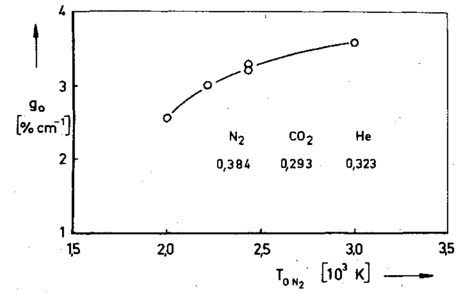

Fig. 1 Variation of small signal gain with stagnation temperature, pure N_2 heated.

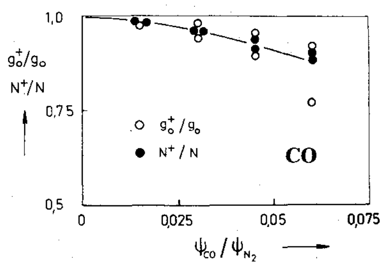

Fig. 2 Normalized small signal gain and laser power vs. CO mole fraction of N_2.

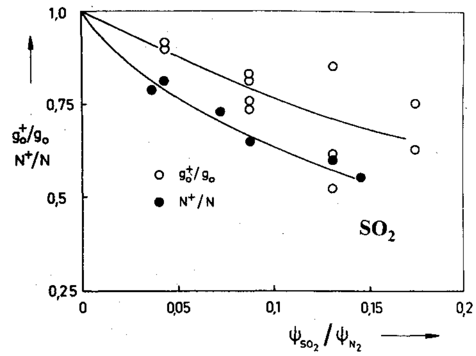

Fig. 3 Normalized small signal gain and laser power vs SO_2 mole fraction of N_2.

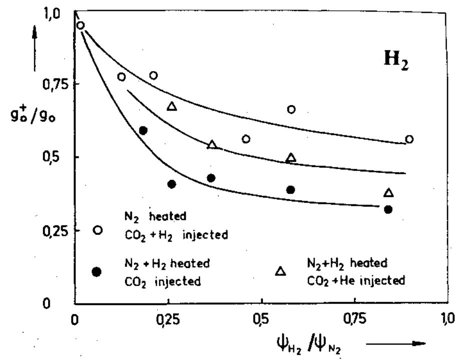

Fig. 4 Small signal gain vs H_2 mole fraction of N_2.

heater yielding typical stagnation conditions of $T_0 \approx 2000$-3000 K and $p_0 \approx 4$-6 bar. The expansion and mixing with the cold CO_2 (pure or premixed with He or H_2) takes place in a screen nozzle. The flow then enters the laser channel of 3.5×1.2 cm^2 cross section. At a distance 8 cm downstream of the nozzle exit measurements of small signal gain g_0 (P20) and laser power N are performed. Figure 1 shows the dependence of g_0 on T_0 if pure N_2 is used. It is noted that at approximately 3000 K values exceeding 3.6 % cm^{-1} are achieved and the curve indicates a further, even though small, rise with increasing temperature. The gas composition, as indicated in the graph, serves as a reference condition. Helium has been used as a deactivating agent throughout the experiments, although its presence is not fundamental for the function of this system. Comparative measurements show a 12% decrease of performance without He.

The various gas additives are heated by injecting them into a plenum chamber. It is of sufficient length to provide good mixing with the primary N_2-flow and to establish well-defined stagnation conditions. Data will be given for $T_0 = 2800$ K.

The effect of CO_2 and H_2O on the deactivation of N_2 is well known and therefore not considered here. The addition of O_2 and NO up to 7.5% to N_2 does not reveal any deteriorating effect on gain and laser power. The effect of CO on the laser performance is shown in Fig. 2. Power and small signal gain are seen to decrease in approximately the same manner. The magnitude of the losses is in good agreement with the findings of Cassady et al.[3]

The results obtained with SO_2 are presented in Fig. 3. Although there is some scatter in the g_0- data at higher mole fractions, the detrimental effect of SO_2 on small signal gain and laser power becomes apparent. The decrease of laser power N^+ (+ indicates conditions with addition of contaminant gases) is noticeably stronger than that of g_0^+. The dependence of g_0^+ on the SO_2 content is about the same as the one that was found in a shock-tube-driven premixed GDL at $T_0 \approx 1500$ K.[5] A definite explanation of this behavior cannot be given at present. However, one has to note the close spacing between the vibrational levels of N_2 at 2331 cm^{-1} and of SO_2 ($2\nu_1$) at 2305 cm^{-1}. It thus appears possible that the energy transfer from N_2 to the upper laser level of CO_2 at 2349 cm^{-1} becomes more inefficient as the number of molecules competing in resonant V–V transfer collisions is increased. Furthermore, the lower laser level of CO_2 at 1388 cm^{-1} is quite close to SO_2 (ν_3) at 1361 cm^{-1} so that an interference with the depopulation process seems conceivable as well.

Finally, experiments have been performed concerning the effects caused by H_2. Some of the results obtained for a wide range of mole fractions are presented in Fig. 4. For the case of H_2 being heated together with N_2 and with pure CO_2 injected into the expanding N_2/H_2 flow, a rather dramatic decrease of small signal gain occurs already for H_2 fractions below 20-25%. Using a mixture of CO_2 and He instead of pure CO_2, the drop in g_0^+ is less pronounced. In addition, a few measurements were made with pure N_2, but He substituted by H_2 and injected together with CO_2. Here too, hydrogen causes a considerable loss of small signal gain, even at a very low H_2 content of about 2%. Both experiments indicate a strong deactivating interference of H_2 with the resonant N_2/CO_2 energy level, whereas no evidence is found for a positive depopulation effect on the lower laser level. All together, these results confirm the generally recognized fact that H_2 has no beneficial effect upon the laser performance.

Conclusion

In conclusion, it is expected that a combustion-driven GDML will preserve its basic advantage of high specific energy as long as the amount of some contaminants (especially SO_2, H_2, H_2O) does not exceed a few percent of the N_2 flow.

References

[1] Taran, J.P.E., Charpenel, M., and Borghi, R., "Investigation of a Mixing CO_2 GDL," AIAA Paper 73-622, Palm Springs, Calif., 1973.

[2] Croshko, V.N., Fomin, N.A., and Solukhin, R.I., "Population Inversion and Gain Distribution in Supersonic Mixed Flow Systems," *Acta Astronautica*, Vol. 2, Nov./Dec. 1975, pp. 929-939.

[3] Cassady, P.E., Newton, J., and Rose, P., "A New Mixing Gasdynamic Laser," AIAA Paper 76-343, San Diego, Calif. 1976.

[4]Schall, W., Hoffmann, P., and Hügel, H., "Performance of N_2/CO_2 Gasdynamic Mixing Lasers with Various Injection Techniques," *Journal of Applied Physics,* Vol. 48, Feb. 1977, pp. 688-690.

[5]Tennant, R., Vargas, R., and Hadley, S., "Effects of Gaseous Contaminants on Gas Dynamic Laser Performance," AIAA Paper 74-178, Washington, D.C., 1974.

Boundary-Layer Blockage with Mass Transfer

Gustave John Hokenson*
STD Research Corporation, Arcadia, Calif.

Nomenclature

b = mass-transfer parameter, $2(\rho v)_w/\rho_e U_e C_{f_0}$
C_f = skin-friction coefficient
F = streamwise variation of channel geometry, Eq. (12)
f_1 = $-2V\times[1-2/b_{\mathrm{cr}_0}]$, Eq. (18)
f_2 = $-2V\times[1+H_1\ (1-2/b_{\mathrm{cr}_0})+(1-M_e^2)\ (\mathrm{d}lnU_e/\mathrm{d}lnx)]$, Eq. (18)
f_3 = $mS_{\mathrm{cr}}\mathrm{d}lnU_e/\mathrm{d}x-\psi\mathrm{d}lnC_{f_0}/\mathrm{d}\theta-2V/C_{f_0}$, Eq. (22)
h = height from wall to channel centerline
H = shape factor, δ^*/θ
M = Mach number
m = constant in Eq. (8), typically 1.75
$\dot{m}$ = mass flow rate
R_e = Reynolds number
S = pressure gradient parameter, $\theta\mathrm{d}lnU_e/\mathrm{d}x$
$\bar{S}$ = S/S_{cr}
U = streamwise velocity
v = transverse velocity
V = $(\rho v)_w/2\rho_e U_e\theta$
W = spanwise channel dimension
x = streamwise coordinate
δ^* = displacement thickness
κ = constant in Eq. (2), typically 0.4
ϵ = pressure gradient parameter, Eqs. (6, 7, and 9)
ρ = fluid density
θ = momentum thickness
ψ = generalized skin friction modulator function
ψ_b = $(1-b/b_{\mathrm{cr}})^2$, constant pressure, isothermal mass transfer ψ
ψ_p = zero mass transfer, isothermal pressure gradient ψ, Eq. (8)

Subscripts

e = freestream conditions
0 = constant pressure, zero mass transfer
1 = variable pressure, zero mass transfer
cr = critical value
w = wall conditions

CONSIDERATION of boundary-layer blockage effects generally involves data correlations or analytical formulations that utilize the local displacement thickness. Internal flows, for example at the entrance to diffusers, and external flows, on slender bodies whose flowfields are dominated by viscous-induced streamline deflection, follow this treatment. In both of these situations, boundary-layer control (suction or blowing) has application in obtaining efficient designs and/or maintaining structural integrity.

Received May 18, 1977; revision received July 12, 1977.
Index category: Boundary Layers and Convective Heat Transfer – Turbulent.

*Senior Scientist and Group Manager, Physical Sciences. Member AIAA.

The δ^* distribution may be obtained through simple integral calculations utilizing the momentum equation

$$\frac{\mathrm{d}\theta}{\mathrm{d}x}+\frac{\theta}{U_e}\frac{\mathrm{d}U_e}{\mathrm{d}x}[H+2-M_e^2]=\frac{C_f}{2}+\frac{(\rho v)_w}{\rho_e U_e} \tag{1}$$

to obtain θ and subsequently $\delta^*=H\theta$.

The results of Ref. 1 provide a method for modeling the effects of pressure gradient and wall temperature on C_f and H in a high-Reynolds-number turbulent flow. The effect of mass transfer on C_f in a constant-pressure isothermal flow also is presented. In addition, an approximate analysis of the influence of mass transfer on C_f in a constant-pressure nonisothermal flow is developed. However, the dependences of H and C_f on mass transfer in a pressure gradient are not addressed.

The purpose of this Note is to point out that, because of the origin of H as a definition based on δ^* and θ, the dependence of H on mass transfer may be exposed directly from considerations of mass continuity. In so doing, it is necessary to utilize only the physical interpretation of δ^* and the fact that mass transfer appears as an explicit term in the momentum equation. A prerequisite to this approach is the development of an appropriate C_f model with mass transfer in a pressure gradient.

Large mass transfer rates are excluded from consideration in order to obtain a closed-form "linearized" solution. This is of particular relevance in diffuser blockage determination, wherein a small amount of system power is diverted to apply suction along a short segment of upstream boundary layer such that the increased diffuser recovery results in a net increase in system efficiency.

The zero-mass-transfer, constant-pressure shape factor is obtained[1] from the relationship

$$H_0=1+\sqrt{2C_{f_0}}/(\kappa-\sqrt{2C_{f_0}}) \tag{2}$$

which extends to variable pressure flows through use of the following endpoint fitting formula:

$$(H_1-1)/(H_0-1)=[(H_{\mathrm{cr}}-1)/(H_0-1)]^{\bar{S}} \tag{3}$$

Both H_0 and H_{cr} are affected by the degree of nonisothermality, as indicated by the results of Ref. 1.

A variety of skin-friction models for constant-pressure flows are available. The formula employed in Ref. 1,

$$C_{f_0}=2.0/(2.5lnRe_\theta+3.8)^2 \tag{4}$$

provides generally useful results for smooth surfaces. Roughness amplification of this value may be obtained from the development in Ref. 2. Inclusion of pressure gradient effects is possible utilizing results from previously computed flows (see Fig. 28 of Ref. 1).

For constant-pressure flows, the combined effects of mass transfer and nonisothermality on C_f are approximated[1] by a superposition of their separate influences. The assumption is made here that the same can be done in variable-pressure flows, and, therefore, isothermal flow is considered for notational clarity.

In constant-pressure flows, the effect of mass transfer on C_f may be written as

$$C_f=C_{f_0}\times\psi_b \tag{5}$$

where ψ_b is obtained from the integration of Eq. (4.2) of Ref. 1. In addition, $b_{\mathrm{cr}}=4.0$, as indicated from the integration when $\psi=0$.

In the presence of pressure gradients, Eq. (5) is inappropriate, and inclusion of a *weak* pressure gradient